Supplemental Information

System-wide benefits of intermeal fasting by autophagy

Nuria Martinez-Lopez#, Elena Tarabra#, Miriam Toledo, Marina Garcia-Macia, Srabani Sahu, Luisa Coletto, Ana Batista-Gonzalez, Nir Barzilai, Jeffrey E. Pessin, Gary J. Schwartz, Sander Kersten, Rajat Singh

Correspondence to:
Rajat Singh, MD, MBBS
Department of Medicine (Endocrinology) and Molecular Pharmacology
Member of the Diabetes Research Center
Albert Einstein College of Medicine
1300 Morris Park Avenue, Forchheimer Building, Room 505D
Bronx, NY 10461 USA
E-mail: rajat.singh@einstein.yu.edu
Phone: 718-430-4118
Fax: 718-430-8557

#Equal contribution

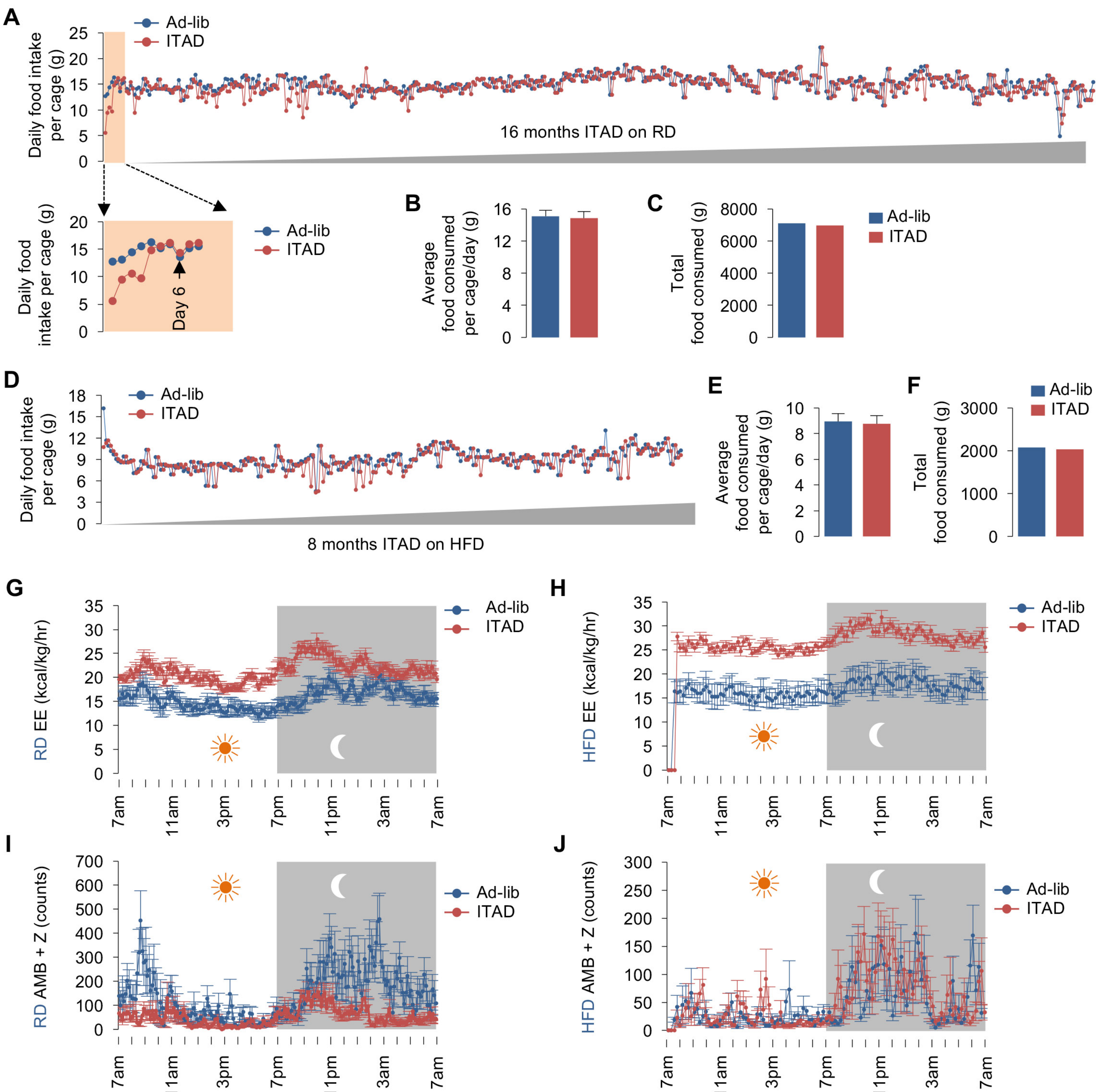

FIGURE S1, related to Figure 1. ITAD feeding and energy expenditure rates

(A-C) Daily food intake, average food consumed per cage per day, and total food consumed per cage over the course of study by group-housed RD-fed male mice on Ad-lib or ITAD feeding for 16mo (n=5).

(D-F) Daily food intake, average food consumed per cage per day, and total food consumed per cage over the course of study by group-housed HFD-fed male mice on Ad-lib or ITAD feeding for 8mo (n=5).

(G) 24 hr energy expenditure (EE) in RD-fed male mice subjected to Ad-lib or ITAD feeding for 16mo (n=5).

(H) 24 hr EE in HFD-fed male mice subjected to Ad-lib or ITAD feeding for 8mo (n=5).

(I) Locomotor activity (ambulation (AMB) and counts in Z-axes) in RD-fed male mice subjected to Ad-lib or ITAD feeding for 16mo (n=5).

(J) AMB and counts in Z-axes in HFD-fed male mice subjected to Ad-lib or ITAD feeding for 8mo (n=5).

All data are expressed as Mean ± S.E.M.

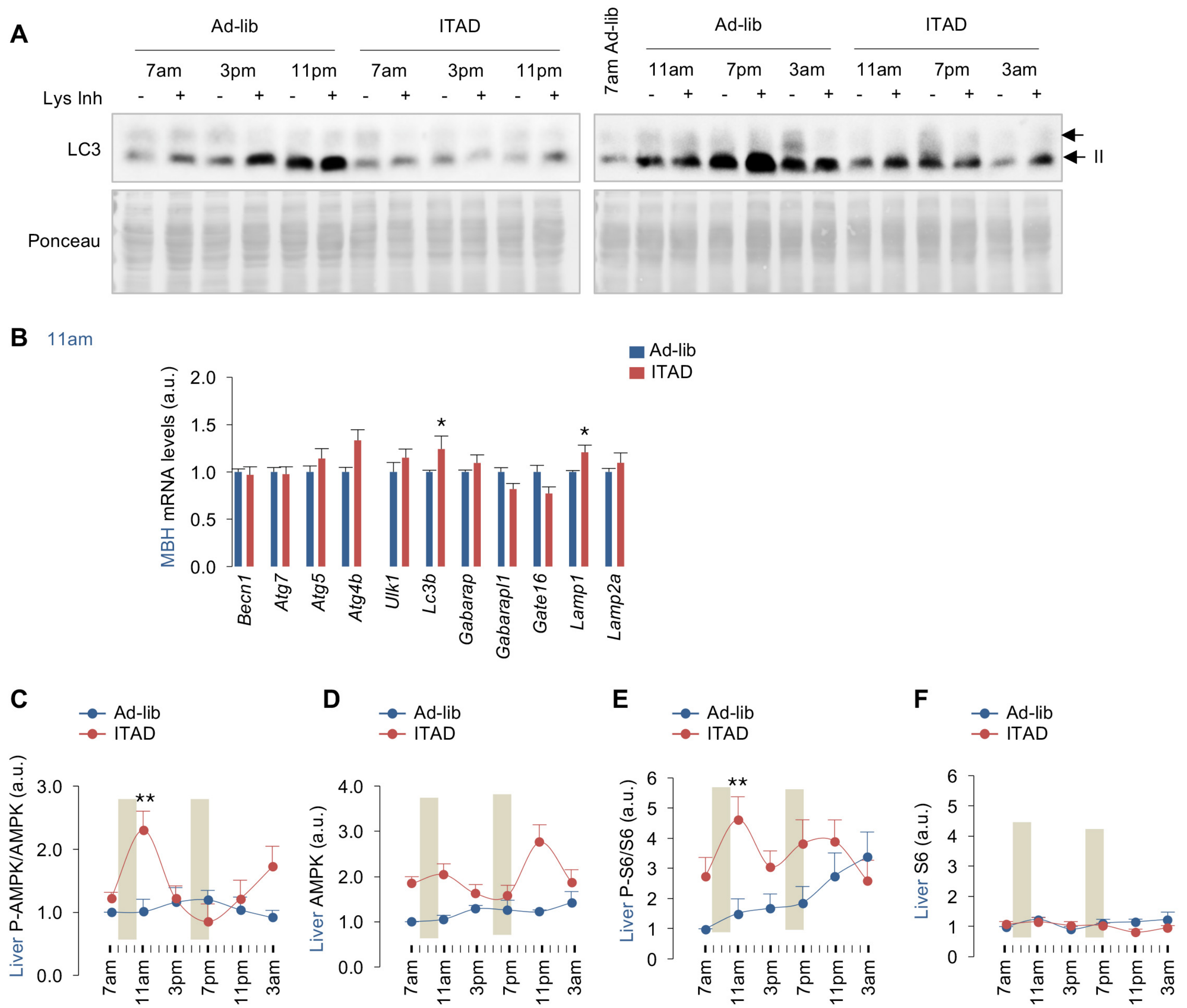

FIGURE S2, related to Figure 2. ITAD feeding and autophagy flux

(A) Immunoblots (IB) for LC3 in liver explants cultured in presence (+) or absence (-) of lysosomal inhibitor (Lys Inh), leupeptin, at indicated time points from male mice fed RD Ad-lib or ITAD for 10mo. Ponceau is the loading control (n=6).

(B) qPCR for indicated autophagy/lysosomal genes in mediobasal hypothalamus (MBH) harvested at 11am from RD-fed male (n=4) and female mice (n=4) on Ad-lib or ITAD for 4mo (pooled total n=8).

(C-F) Densitometry of IB for indicated proteins across 24 hr in livers from RD-fed male mice fed Ad-lib or ITAD for 10mo (n=6).

All data are expressed as Mean ± S.E.M. ∗$p<0.05$, Student's t test. For multiple comparisons, we used Two-Factor ANOVA and Bonferroni multiple comparison test.

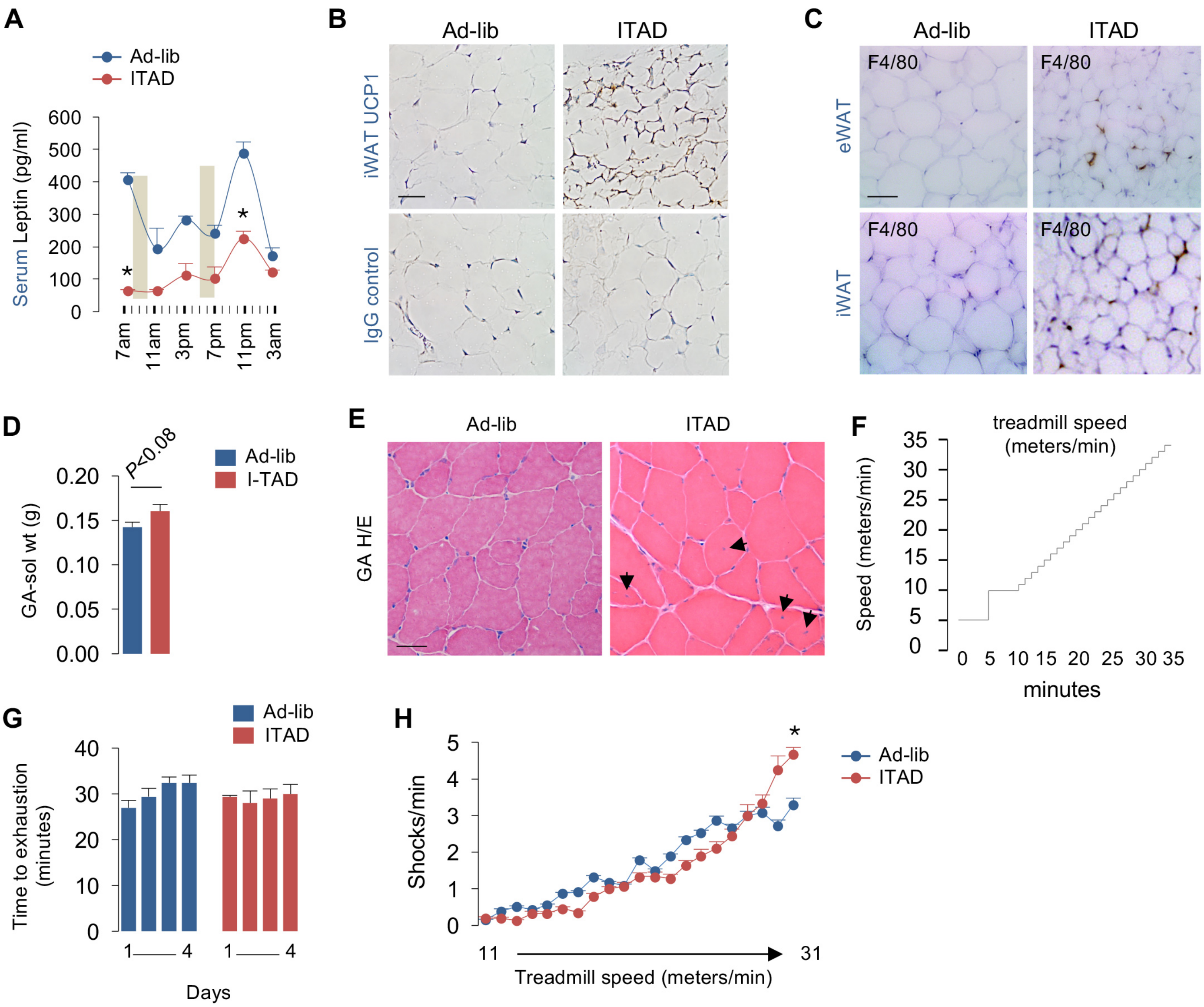

FIGURE S3, related to Figure 3. ITAD feeding remodels adipose tissue and skeletal muscle
(A) Serum leptin at indicated time points in RD-fed male mice on Ad-lib or ITAD for 10mo (n=3).
(B-C) IHC for UCP1 and F4/80 in indicated fat tissue from RD-fed male mice on Ad-lib or ITAD feeding for 9mo (n=3-5). For panel B: IgG-only control sections are also shown.
(D-E) Muscle (Gastrocnemius-soleus (GA-sol)) wt, and H/E stains for GA from the same group of RD-fed male mice fed Ad-lib or ITAD for 9mo (n=4). Arrowheads indicate centralized nuclei.
(F) Treadmill exercise protocol for test of endurance depicting a start speed of 5 meters/min for 5 min, followed by increase in speed to 10 meters/min for 5 min, which is followed by increments in speed every min by 1 meter/min until the onset of exhaustion determined by the inability to stay on the treadmill despite shocks.
(G) Quantification for the time to exhaustion on days 1-4 when RD-fed male mice on Ad-lib or ITAD feeding for 11mo were acclimatized to the treadmill (n=3-5).
(H) Treadmill endurance capacity in RD-fed male mice on Ad-lib or ITAD for 11mo (n=3-5).
All data are expressed as Mean ± S.E.M. $*p<0.05$, Student's t test. For multiple comparisons, we used Two-Factor ANOVA and Bonferroni multiple comparison test. Scale: 50μm.

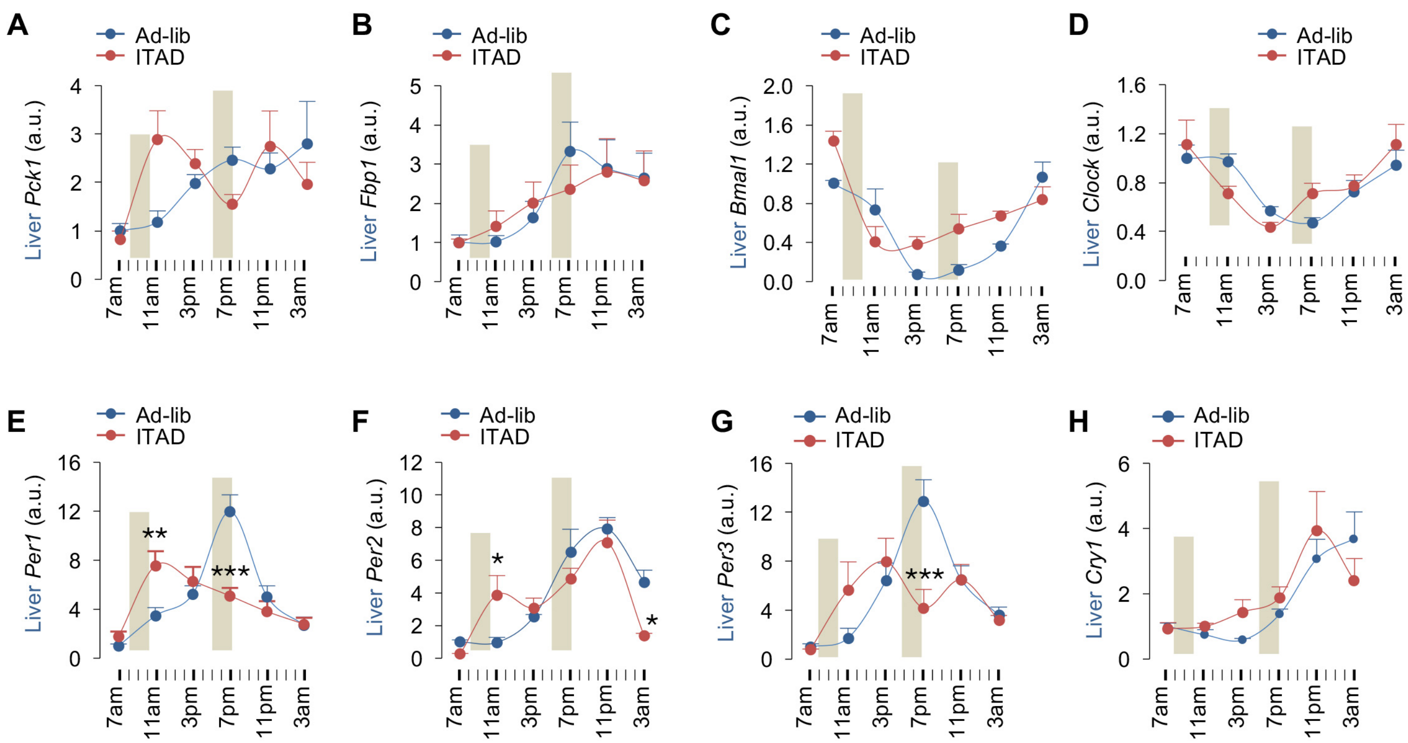

FIGURE S4, related to Figure 4. ITAD feeding and its relation to glucose metabolism and circadian rhythm
(A-H) qPCR for indicated genes across 24 hr in livers from male RD-fed mice subjected to Ad-lib or ITAD feeding for 10mo (n=8).
All data are expressed as mean ± S.E.M. *P<0.05, **P<0.01, ***P<0.001. Two-way ANOVA and Bonferroni multiple comparison test.

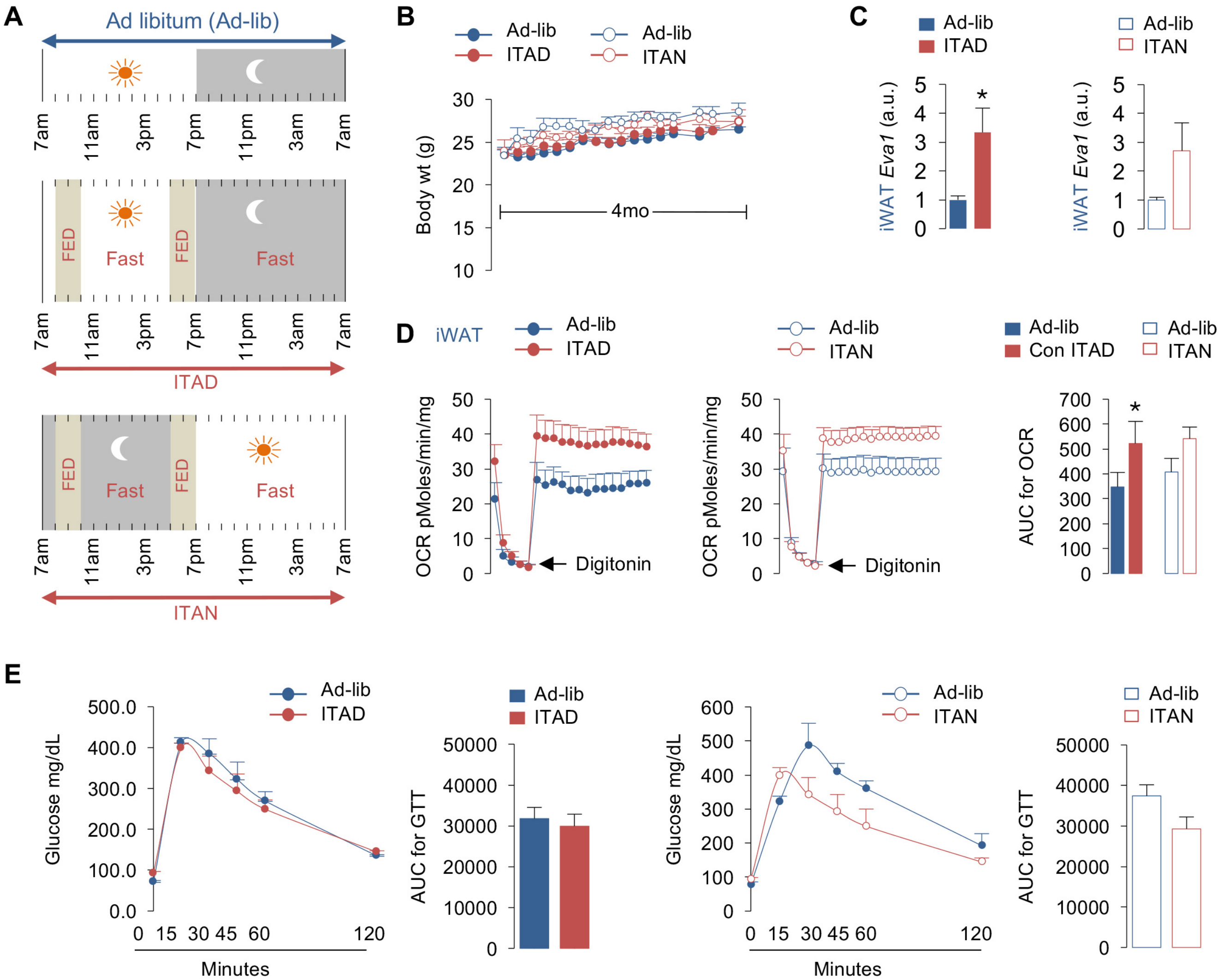

FIGURE S5, related to Figure 4. ITAD feeding compared to ITAN feeding
(A) Cartoon depicting plan for ITAD feeding or isocaloric twice a night (ITAN) feeding.
(B) Body wt in RD-fed male mice subjected to Ad-lib, ITAD or ITAN feeding for 4mo (n=3).
(C) *Eva1* gene expression in iWAT in RD-fed male mice subjected to Ad-lib, ITAD or ITAN feeding for 4mo (n=5).
(D) iWAT OCR and AUC for OCR in RD-fed male mice subjected to Ad-lib, ITAD or ITAN feeding for 4mo (n=5).
(E) GTT and AUC for GTT in RD-fed male mice subjected to Ad-lib, ITAD or ITAN feeding for 4mo, n=3-6.
All data are expressed as Mean ± S.E.M. *p<0.05, Student's t test. For multiple comparisons, we used Two-Factor ANOVA and Bonferroni multiple comparison test.

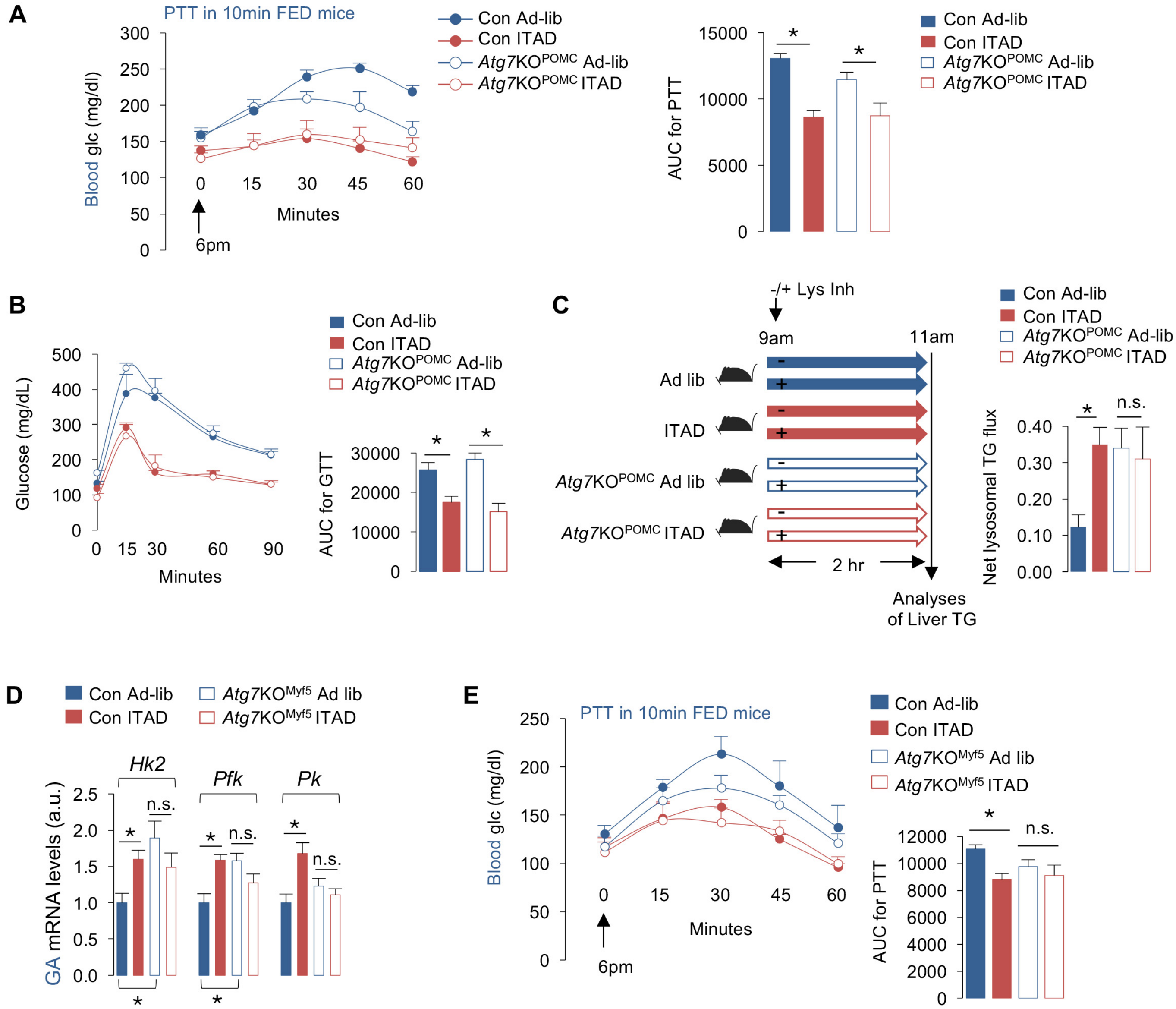

FIGURE S6, related to Figure 6. Tissue-specific autophagy and metabolic benefits of ITAD feeding
(A) Pyruvate tolerance test (PTT) and AUC in RD-fed Con and *Atg7*KO^{POMC} male (n=4) and female mice (n=4) subjected to ITAD feeding for 4mo (pooled total n=8).
(B) GTT in HFD-fed Con and *Atg7*KO^{POMC} male mice fed Ad-lib or ITAD for 4mo (n=4).
(C, left) Experimental plan to test for the requirement of POMC neuronal autophagy in lysosomal fat depletion in liver in response to ITAD feeding. Livers collected at 11am from HFD-fed control (Con) and *Atg7*KO^{POMC} mice subjected to Ad-lib or ITAD feeding for 4mo and injected i.p. or not with leupeptin for 2 hr prior to sacrifice. Livers were then analyzed for TG.
(C, right) Net lysosomal TG flux in liver explants (net TG flux = TG from lysosomal inhibitor-treated liver – TG from inhibitor-untreated liver) from HFD-fed control (Con) and *Atg7*KO^{POMC} male (n=4) and female mice (n=4) mice fed Ad-lib or ITAD feeding for 4mo (pooled total n=8).
(D) qPCR analyses for indicated genes in GA from Con and *Atg7*KO^{Myf5} male (n=3) and female mice (n=3) fed RD Ad-lib or ITAD for 6mo (pooled total n=6).
(E) PTT in RD-fed Con and *Atg7*KO^{Myf5} male (n=3) and female mice (n=3) subjected to ITAD for 4mo (pooled total n=6).
All data are expressed as Mean ± S.E.M. ∗p<0.05. Two-way ANOVA and Bonferroni multiple comparison test.

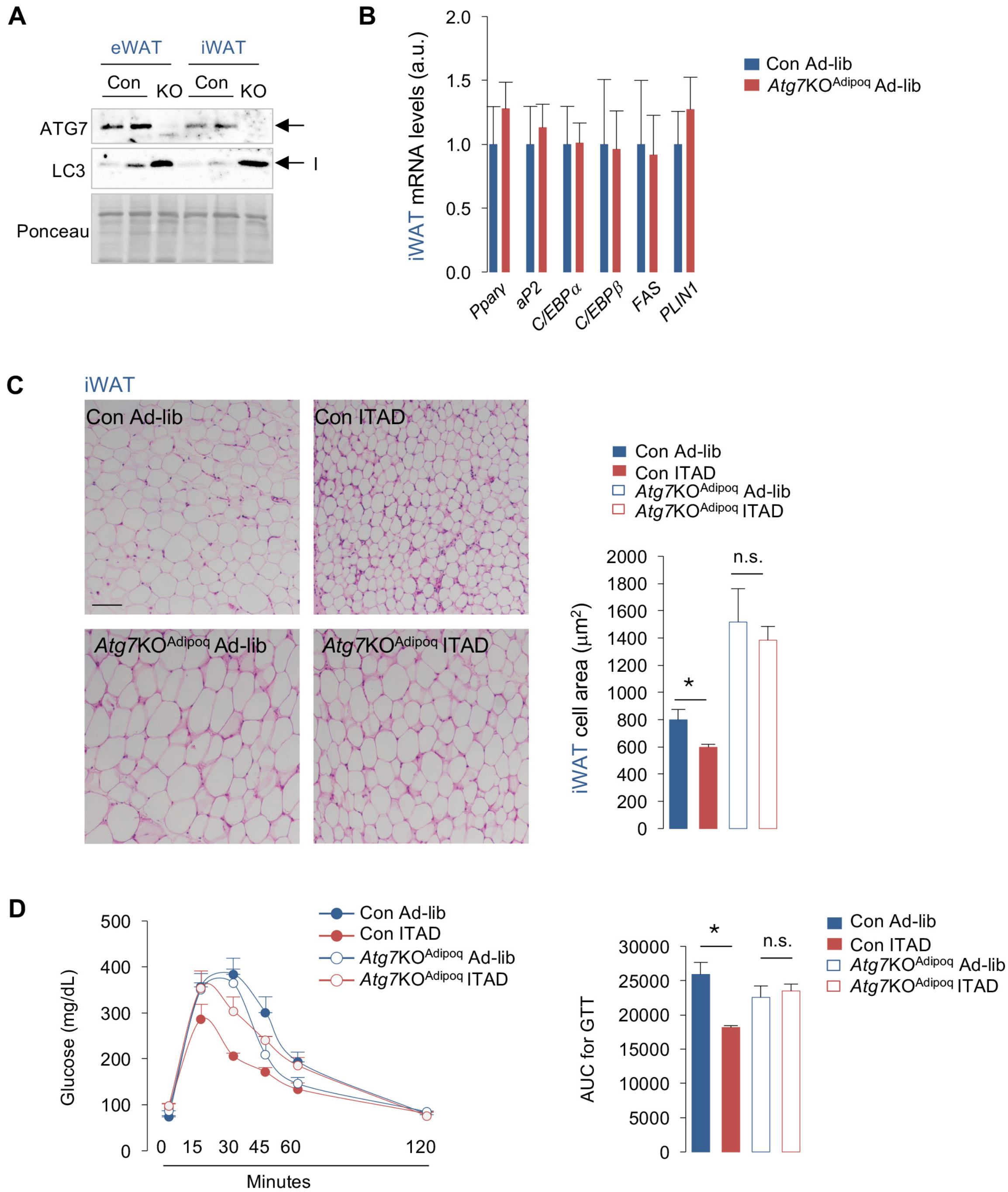

FIGURE S7, related to Figure 7. Adipose autophagy and ITAD feeding-driven adipose remodeling

(A) IB for indicated proteins in eWAT and iWAT from Con and *Atg7*KO^{Adipoq} male mice. Ponceau is the loading control.

(B) qPCR for indicated adipocyte differentiation markers in Ad-lib RD-fed Con and *Atg7*KO^{Adipoq} male (n=3) and female (n=3) mice (pooled total n=6).

(C) Representative H/E sections of iWAT from Con and *Atg7*KO^{Adipoq} male (n=3) and female (n=3) mice subjected to Ad-lib or ITAD feeding on HFD for 4mo (pooled total n=6). Quantification for adipocyte size (adipocyte area in μm^2) is shown.

(D) Glucose tolerance test (GTT), and area under curve (AUC) for GTT in Con and *Atg7*KO^{Adipoq} mice subjected to Ad-lib or ITAD feeding on HFD for 4mo in male (n=3) and female (n=3) mice (pooled total n=6).

All data are expressed as Mean ± S.E.M. ∗p<0.05, ∗∗p<0.01, Two-way ANOVA and Bonferroni correction. Scale: 100μm.

TABLE S1. Primers for real-time PCR analysis related to STAR Methods

GENE	PROTEIN	PRIMERS
Acc1	Acetyl-Coenzyme A carboxylase	(f) 5'-ctggagctaaaccagcactcccgat-3' (r) 5'-gagctgacggaggctggtgaca-3'
Acsl5	Acyl-CoA synthetase long-chain family member 5	(f) 5'-gatcggggtaaagggatcat-3' (r) 5'-ggcaagctctactcgtttgg-3'
Arntl	Aryl hydrocarbon receptor nuclear translocator like	(f) 5'-aaatccacaggataagaggg-3' (r) 5'-atagtccagtggaaaggaatg-3'
Atg4b	Autophagy related 4B cysteine peptidase	(f) 5'-tgggtgttattggagggaag-3' (r) 5'-cagaaaaaccccacagcaat-3'
Atg5	Autophagy related 5	(f) 5'-tagaatatatcagaccacgacg-3' (r) 5'-ctcctcttctctccatcttc-3'
Atg7	Autophagy related 7	(f) 5'-tccgttgaagtcctctgctt-3' (r) 5'-ccactgaggttcaccatcct-3'
Becn1	Beclin 1	(f) 5'-ggccaataagatgggtctga-3' (r) 5'-gctgcacacagtccagaaaa-3'
Ckm	CKM creatine kinase, M-type	(f) 5'-catggagaagggaggcaata-3' (r) 5'-gacgaaggcgagtgagaatc-3'
Clock	Circadian locomotor output cycles kaput	(f) 5'-aagtgactcattaacccctg-3' (r) 5'-ctatgtgtgcgttgtatagttc-3'
Cox4	Cytochrome c oxidase subunit 4	(f) 5'-gccccatccctcatactttc-3' (r) 5'-gctctcacttcttccactcattct-3'
Cry1	Cryptochrome 1	(f) 5'-agaagggatgaaggtctttg-3' (r) 5'-ctcttaggacaggtaaataacg-3'
Cpt1b	Carnitine palmitoyltransferase 1B	(f) 5'-agtttgtcctgggcactgatacct-3' (r) 5'-tgccttggctacttggtacgagtt-3'
Cpt2	Carnitine palmitoyltransferase 2	(f) 5'-cctgatggctttggcattgcgtat-3' (r) 5'-acagtggagaaactctcgggcatt-3'
CyclinA1	Cyclin 1	(f) 5'-ttccccaatgctggttga-3' (r) 5'-aaccaaaatccgttgcttcct-3'
CyclinD1	Cyclin D1	(f) 5'-tctacactgacaactctatccg-3' (r) 5'-tctacactgacaactctatccg-3'
Ebf2	Early B-cell factor 2	(f) 5'-gctgcgggaaccggaacgaga-3' (r) 5'-acacgacctggaaccgcctca-3'
Elovl6	ELOVL family member 6	(f) 5'-cgtagcgactccgaagatcagcc-3' (r) 5'-agcgtacagcgcagaaaacagga-3'
Eva1	Myelin protein zero like 2	(f) 5'-ccacttctcctgagtttacagc-3' (r) 5'-gcattttaaccgaacatctgtcc-3'
F4/80	Adhesion G protein-coupled receptor E1	(f) 5'-ccacttctcctgagtttacagc-3' (r) 5'-gcattttaaccgaacatctgtcc-3'
Fas	Fatty acid synthase	(f) 5'-cactgcattgacggccgggt-3' (r) 5'-ggacaagcccaggctgcgag-3'
Fbpase	Fructose bisphosphatase 1	(f) 5'-ctgctgaattcgctctgcac-3' (r) 5'-ggttgagccagcgataccat-3'
Fbxo31	F-box protein 31	(f) 5'-aaactgcttcaccgatacagac-3' (r) 5'-accacgacgttcagcaatcc-3'
Fgf21	Fibroblast growth factor 21	(f) 5'-agatcagggaggatggaaca-3' (r) 5'-tcaaagtgaggcgatccata-3'
G6Pase	Glucose-6-phosphatase	(f) 5'-gtttggtttcgcgcttggat-3' (r) 5'-gccgctcacaccatctctta-3'
Gabarap	Gamma-aminobutyric acid receptor associated protein	(f) 5'-gtcccggtgatagtggaaaa-3' (r) 5'-tgggtggaatgacattgttg-3'
Gabarapl1	Gamma-aminobutyric acid A receptor-associated protein-like 1	(f) 5'-tcgtggagaaggctcctaaa-3' (r) 5'-atacagctggcccatggtag-3'
Gabarapl2	Gamma-aminobutyric acid A receptor-associated protein-like 2	(f) 5'-tctcgggctctcagattgtt-3' (r) 5'-gtgttctctccgctgtaggc-3'

Gpat1	Gycerol-3-phosphate acyltransferase 1	(f) 5’-tgccggtgcacagatcccac-3’ (r) 5’-cggcgccttgatgttgtggc-3’
Hk2	Hexokinase 2	(f) 5’-cgtgtccctacctttgggtt-3’ (r) 5’-ccaggtcaaactcctctcgc-3’
IL-1β	Interleukin 1 beta	(f) 5’-aagggctgcttccaaacctttgac-3’ (r) 5’-atactgcctgcctgaagctcttgt-3’
IL-4	Interleukin 4	(f) 5’-atggagctgcagagactctt-3’ (r) 5’-aaagcatggtggctcagtac-3’
IL-6	Interleukin 6	(f) 5’-gctaaggaccaagaccatccaat-3’ (r) 5’-gcttaggcataacgcactaggttt-3’
IL-10	Interleukin 10	(f) 5’-ggttgccaagccttatcgga-3’ (r) 5’-acctgctccactgccttgct-3’
IL-13	Interleukin 13	(f) 5’-cagcatggtatggagtgtgg-3’ (r) 5’-tgggctacttcgattttggt-3’
iNOS	Nitric oxide synthase 2, inducible	(f) 5’-ggcagcctgtgagacctttg-3’ (r) 5’-gcattggaagtgaagcgtttc-3’
Klhl3	Kelch like family member 3	(f) 5’-agaattggttgctgcaatactcc-3’ (r) 5’-aaggcacagtttcaagtgctg-3’
Lamp1	Lysosomal associated membrane protein 1	(f) 5’-tagtgcccacattcagcatctcca-3’ (r) 5’-ttccacagacccaaacctgtcact-3’
Lamp-2a	Lysosomal-associated membrane protein 2A	(f) 5’-aggtgctttctgtgtctagagcgt-3’ (r) 5’-agaataagtactcctcccagagctgc-3’
Lc3b	Microtubule associated protein 1 light chain 3 beta	(f) 5’-acaaagagtggaagatgtccggct-3 (r) 5’-tgcaagcgccgtctgattatcttg-3’
Myf5	Myogenic factor 5	(f) 5’-agacgcctgaagaaggtcaa-3’ (r) 5’-gttctccacctgttccctca-3’
Myf6	Myogenic factor 6	(f) 5’-atggtaccctatccccttgc-3’ (r) 5’-tagctgctttccgacgatct-3’
Myod1	Myogenic differentiation 1	(f) 5’-agtgaatgaggccttcgaga-3’ (r) 5’-gcatctgagtcgccactgta-3’
Myog	Myogenin	(f) 5’-ctacaggccttgctcagctc-3’ (r) 5’-acgatggacgtaagggagtg-3’
Nd1	NADH dehydrogenase, subunit 1 (complex I)	(f) 5’-tgtggaagaagcagatgttg-3’ (r) 5’-aagacctcgcagaatgaatg-3’
Pax3	Paired box 3	(f) 5’-aaacccaagcaggtgacaac-3’ (r) 5’-ctagatccgcctcctcctct-3’
Pax7	Paired box 7	(f) 5’-gagttcgattagccgagtgc-3’ (r) 5’-cgggttctgattccacatct-3’
Pck1	Phosphoenolpyruvate carboxykinase 1	(f) 5’-cttgctctaccgtgagcctc-3’ (r) 5’-accacaatcaccagatcacc-3’
Pdgfrα	Platelet derived growth factor receptor, alpha polypeptide	(f) 5’-caccggatggtacacttgct-3’ (r) 5’-gtcatcccgagaggcacaaa-3’
Per1	Period circadian clock 1	(f) 5’-gttctcatagttcctcttctg-3’ (r) 5’-gtgagtttgtactcttgctg-3’
Per2	Period circadian clock 2	(f) 5’-ctttcactgtaagaaggacg-3’ (r) 5’-ctgagtgaaagaatctaagcc-3’
Per3	Period circadian clock 3	(f) 5’-gagagtatgtcattctggattc-3’ (r) 5’-tcatttaatggactcgttcg-3’
Pfk	Phosphofructokinase	(f) 5’-ggagagctaaaactacaagagtgga-3’ (r) 5’-cgcccgtgaagataccaact-3’
Pgc1α	Peroxisome proliferative activated receptor, gamma, coactivator 1 alpha	(f) 5’-ccctgccattgttaagacc-3’ (r) 5’-tgctgctgttcctgttttc-3’
Pk	Pyruvate kinase	(f) 5’-atgcagcacctgatagctcg-3’ (r) 5’-aggtctgtggagtgactgga-3’
Pparα	Peroxisome proliferator activated receptor alpha	(f) 5’-gcgtacggcaatggctttat-3’ (r) 5’-gaacggcttcctcaggttctt-3’
Pparɣ	Peroxisome proliferator activated receptor gamma	(f) 5’-ttttcaagggtgccagtttc-3’ (r) 5’-aatccttggccctctgagat-3’

Scd1	Stearoyl-Coenzyme A desaturase 1	(f) 5’-tcatcccatcgcctgctctaccc-3’ (r) 5’-tggtgtaggcgagtggcggaa-3’
Srebp1c	Sterol regulatory element binding transcription factor 1	(f) 5’-ccagcggctgccttcacaca-3’ (r) 5’-ccagccgaaaagcgaggcca-3’
Tbp	TATA-box binding protein	(f) 5’-gaagctgcggtacaattccag-3’ (r) 5’-ccccttgtacccttcaccaat-3’
Tbx1	T-box 1	(f) 5´-ggcaggcagacgaatgttc-3´ (r) 5´-ttgtcatctacgggcacaaag-3’
Tmem26	Transmembrane protein 26	(f) 5´-accctgtcatcccacagag-3´ (r) 5´-tgtttggtggagtcctaaggtc-3’
Tnfα	Tumour necrosis factor alpha	(f) 5’-cgtcagccgatttgctatct-3’ (r) 5’-cggactccgcaaagtctaag-3’
Ucp1	Uncoupling protein 1	(f) 5’-actgccacacctccagtcatt-3’ (r) 5’-ctttgcctcactcaggattgg-3’
Ulk1	Unc-51 like autophagy activating kinase 1	(f) 5’-agattgctgactttggattc-3’ (r) 5’-agccatgtacataggagaac-3’
Ym1	Chitinase-like 3	(f) 5’-actttgatggcctcaacctg-3’ (r) 5’-aatgattcctgctcctgtgg-3’
Zic1	Zinc finger protein of the cerebellum 1	(f) 5’-aacctcaagatccacaaaagga-3’ (r) 5’-cctcgaactcgcacttgaa-3’